Cranfield

College of Aeronautics Report 8311
May 1983

Stiffness changes in unidirectional composites caused by crack systems

by N. Laws, G. J. Dvorak, and M. Hejazi

College of Aeronautics
Cranfield Institute of Technology
Cranfield, Bedford, UK

Cranfield

College of Aeronautics Report 8311
May 1983

Stiffness changes in unidirectional composites caused by crack systems

by N. Laws, G. J. Dvorak, and M. Hejazi

College of Aeronautics
Cranfield Institute of Technology
Cranfield, Bedford, UK

ISBN 0902937 90 1

£7.50

I. INTRODUCTION

Fibrous composite structures which are subjected to monotonic or cyclic loading frequently develop internal matrix cracks which adversely affect overall stiffness and strength. This phenomenon has been widely observed in laminated plates, where individual layers are found to contain their own systems of cracks. Typical crack systems appear to consist of many parallel cracks on planes which are perpendicular to the midplane of the layer and parallel to the fiber direction. Experimental observations of such internal cracks have been made by Dvorak and Johnson [1,2] in metal matrix B-Aℓ laminates, by Reifsnider et al., [3], Bader et al., [4], and by several other authors in certain polymer matrix composites. Although the geometry of the crack system appears to be similar in both metal and polymer matrix laminates the response to loading is different. Polymer matrix composites start to crack at low strain levels, under both monotonic and cyclic loads. On the other hand metal matrix composites usually deform plastically and do not exhibit extensive matrix cracking under monotonic loads, but are quite susceptible to matrix fatigue cracking when cycled outside the shakedown range [1]. In addition to matrix cracking, all composite systems contain many other damage modes, such as fiber breaks, and delamination cracking between layers. However, these modes appear to be significant at relatively high loads which usually exceed allowable design magnitudes.

Matrix cracking is present at low loads and should be accounted for in structural design.

Certain composite systems also permit crack growth in the matrix on planes which are perpendicular to the fiber axis. Specific examples of this type of cracking have been observed by White and Wright [5] and by Dvorak and Johnson [2] in zero-degree plies of laminated and unidirectional B-Aℓ plates. In such composite systems the fibres remain undamaged while the cracks propagate in the soft matrix between the fibres.

In this paper we are concerned with the development of constitutive equations for fibrous composites which contain a family of longitudinal slit cracks. The theory is also valid for transverse cracks but detailed study of such cracks is deferred to a subsequent paper. In general, we assume that the cracks and fibers have diameters of similar size and that there is mutual interaction. We also investigate the special case of small diameter fibers and large cracks. The overall elastic moduli and compliances of each cracked fibrous composite are obtained from a variant of the self-consistent method.

The approach to the problem is quite similar to that which is often followed in the evaluation of overall moduli of fibrous composites without cracks. Therefore, it is expected that the results may be utilized in evaluation of macroscopic stiffness changes caused by crack systems in laminated plates. To a first approximation, one may regard the properties of the infinite cracked medium of Figure 1a as identical to those of a cracked lamina, Figure 1b. However, when the fiber diameter is much smaller than the crack length, the fibers and matrix in Figure 1a may be replaced by an effective homogeneous medium which in turn contains cracks of half-length a. Again, the stiffness of this cracked medium can be used to describe the properties of a cracked lamina, Figure 1c.

We are not concerned here with a laminate analysis but note that the transition from the configuration of Figure 1a to that of Figures 1b or 1c poses some unresolved problems. Nevertheless, we recall that in the evaluation of the elastic properties of monolayer laminates reinforced by large diameter fibers, such as boron, the transition between the fibre configurations shown in Figures 1a and 1b is commonly accepted. These and other related topics will be dealt with in a subsequent paper on cracked laminates.

We note that related work on the evaluation of overall moduli of cracked <u>homogeneous</u> solids has previously been reported by Bristow [6], Walsh [7], Budiansky and O'Connell [8], Hoenig [9] and Willis [10]. It is also appropriate to mention the work of Taya and Mura [11] on the effect of penny-shaped fiber-end cracks on the overall stiffness of short fiber reinforced composites.

Finally we recall that the paper by Delameter et al [12] describes the effect of the presence of a rectangular array of cracks on the response of an elastic solid. Since Delameter et al [12] consider a solid whose statistics exhibit long-range order, it is difficult to compare their work with the more common approaches which involve homogeneous statistics without long-range order.

The plan of this paper is as follows. In Section 2 we give a brief account of the self-consistent model of a composite. Section 3 contains a detailed description of how the model may be applied to a fibrous composite containing a family of longitudinal slit cracks. Each crack is modelled as the limit of an elliptic cylinder when the aspect ratio tends to zero. We are thus led to a <u>three phase model</u> for cracked fibrous composites. As has already been discussed, there are situations in which the fiber diameter is much smaller than the crack length. Correspondingly we derive a <u>two phase model</u> in which the cracks are present in an effective medium. This two phase model is investigated in Section 4 wherein it is shown that the required equations reduce to a particularly simple form. The paper concludes with some detailed numerical results for selected systems.

2. GOVERNING EQUATIONS

We follow an established pattern in the theory of composite materials and use a notation introduced by Hill [13]. Fourth order Cartesian tensors are denoted by upper case letters, e.g., L, Λ, and symmetric second order tensors are denoted by lower case bold face letters, e.g., $\underset{\sim}{\sigma}$, $\underset{\sim}{\varepsilon}$. The unit fourth order tensor is denoted by I and the inverse of a nonsingular fourth order tensor A is denoted by A^{-1}.

In this paper we make extensive use of the solution of an inclusion problem for an elliptic cylinder in an anisotropic elastic medium. Consider a linear elastic solid in which the stress tensor $\underset{\sim}{\sigma}$, and linear strain tensor $\underset{\sim}{\varepsilon}$ are related through constitutive equations

$$\underset{\sim}{\sigma} = L\underset{\sim}{\varepsilon} \;, \qquad \underset{\sim}{\varepsilon} = M\underset{\sim}{\sigma} \;, \qquad LM = ML = I \;, \tag{1}$$

where L and M are the stiffness and compliance tensors, respectively. Suppose that an infinite homogeneous solid contains an elliptic cylindrical inclusion

$$\frac{x_1^2}{a^2} + \frac{x_2^2}{b^2} = 1 \;, \qquad |x_3| < \infty \quad . \tag{2}$$

The elastic properties of the inclusion are identical to those of the surrounding medium, Equation (1), but the inclusion is subjected to a certain uniform transformation strain. It is known that the solution of this problem requires the determination of the tensor P whose components are given by [14], or [15 ,Equations (9) and (10)$^{+}$] :

$$P_{ijk\ell} = \frac{ab}{8\pi}\int_{0}^{2\pi} \frac{(\omega_i f_{jk}\omega_\ell + \omega_j f_{ik}\omega_\ell + \omega_i f_{j\ell}\omega_k + \omega_j f_{i\ell}\omega_k)}{(a^2\omega_1^2 + b^2\omega_2^2)}\, d\psi \quad , \tag{3}$$

where $\omega_1 = \cos\psi$, $\omega_2 = \sin\psi$, and f_{ik} is the matrix inverse of $L_{ijk\ell}\omega_j\omega_\ell$.

It is often convenient to work with the tensor Q which is defined by

$$Q = L - LPL \quad . \tag{4}$$

Consider now an elliptic cylinder, with stiffness L_r and compliance M_r, which is embedded in an infinite matrix whose stiffness and compliance tensors are, respectively, L and M. The matrix is loaded by uniform stress, $\underset{\sim}{\bar{\sigma}}$, or subjected to uniform strain, $\underset{\sim}{\bar{\varepsilon}}$, at infinity. Let the stress and strain fields in the inclusion be $\underset{\sim}{\sigma}_r$ and $\underset{\sim}{\varepsilon}_r$ respectively, so that

$$\underset{\sim}{\sigma}_r = L_r \underset{\sim}{\varepsilon}_r \quad , \qquad \underset{\sim}{\varepsilon}_r = M_r \underset{\sim}{\sigma}_r \quad .$$

It is well known that the elastic field in the ellipsoidal inclusion is uniform [17,18] and can be evaluated as

+ Note that a factor 4 is missing from the right hand side of (10).

$$\underset{\sim}{\varepsilon}_r = \left[I + P(L_r - L)\right]^{-1} \bar{\underset{\sim}{\varepsilon}} \quad , \tag{5}$$

$$\underset{\sim}{\sigma}_r = \left[I + Q(M_r - M)\right]^{-1} \bar{\underset{\sim}{\sigma}} \quad . \tag{6}$$

Turning now to the basic equations for composites, we note that in order that the concept of overall moduli be meaningful, it is essential to consider macroscopically uniform loading [13,16]. In such circumstances the applied stress is equal to the average stress, $\bar{\underset{\sim}{\sigma}}$, and the phase average stresses, $\bar{\underset{\sim}{\sigma}}_r$ and strains, $\bar{\underset{\sim}{\varepsilon}}_r$, are related to the overall averages through

$$\bar{\underset{\sim}{\varepsilon}}_r = A_r \bar{\underset{\sim}{\varepsilon}} \ , \qquad \bar{\underset{\sim}{\sigma}}_r = B_r \bar{\underset{\sim}{\sigma}} \ . \tag{7}$$

Let c_r denote the volume concentration of the rth phase and let L_r and M_r respectively denote the stiffness and compliance of the rth phase. Since

$$\sum c_r = 1 \quad , \quad \bar{\underset{\sim}{\sigma}} = \sum c_r \bar{\underset{\sim}{\sigma}}_r \quad , \quad \bar{\underset{\sim}{\varepsilon}} = \sum c_r \bar{\underset{\sim}{\varepsilon}}_r \quad , \tag{8}$$

it follows [13] that the overall stiffness L and compliance M are given by

$$L = \sum c_r L_r A_r \quad , \quad M = \sum c_r M_r B_r \quad . \tag{9}$$

Finally we recall that the self-consistent method furnishes estimates of the strain and stress concentration factors A_r, B_r through the solution of the auxiliary inclusion problem in which a typical fiber is embedded in the effective overall medium. In fact from (5), (6) and (7) we can read off the self-consistent estimates

$$A_r = \left[I + P(L_r - L)\right]^{-1} \quad , \tag{10}$$

$$B_r = \left[I + Q(M_r - M)\right]^{-1} \quad . \tag{11}$$

We emphasize that the P and Q tensors appearing in (10) and (11) depend upon the aspect ratio of the considered inclusion and the stiffness of the effective medium L.

3. A FIBROUS COMPOSITE CONTAINING LONGITUDINAL CRACKS

3.a. Three Phase System

We are interested in the elastic response of a composite consisting of a continuous matrix reinforced by a family of parallel fibers in the x_3 direction. Because of past loading, the composite also contains a homogeneous distribution of parallel slit cracks which are aligned in the direction of the fibers. Cartesian coordinate axes are chosen so that the x_2-axis is the common normal to all crack planes, c.f, Figure 1a. We assume that such cracks can be modelled by taking the limit of the elliptic cylinder (2) as the aspect ratio

$$\delta = b/a \tag{12}$$

tends to zero. Thus we consider a mixture of three homogeneous phases. Let phase 1 refer to the fibers, phase 2 to the matrix, and phase 3 to another set of elliptical fibers. Ultimately we will choose phase 3 to consist of voids, and, in the limit $\delta \to 0$, of cracks.

As emphasized by Walsh [7] , the passage from a general two (or three) phase medium to a cracked solid must be achieved by first taking one component to be vacuous and then allowing the aspect ratio to vanish. The reverse procedure leads to erroneous results. Of course, if we had started with a solid containing voids, the double limit problem would not have arisen.

The overall stiffness and compliance tensors for the three-phase medium follow from (9):

$$L = c_1L_1A_1 + c_2L_2A_2 + c_3L_3A_3 \quad , \quad M = c_1M_1B_1 + c_2M_2B_2 + c_3M_3B_3 \; . \tag{13}$$

Also, from (7) and (8)

$$c_1A_1 + c_2A_2 + c_3A_3 = I \; , \quad c_1B_1 + c_2B_2 + c_3B_3 = I \; . \tag{14}$$

It is convenient to use (14) to eliminate the concentration factors for the matrix (r=2) from (13), to give

$$L = L_2+c_1(L_1-L_2)A_1+c_3(L_3-L_2)A_3 , \quad M = M_2+c_1(M_1-M_2)B_1+c_3(M_3-M_2)B_3 . \tag{15}$$

In this application of the self-consistent method we are interested in three-phase materials in which the two families of parallel fibers have different geometries. Correspondingly, we need to account for the different aspect ratios of the two families of fibers.

Thus, let P_1 and Q_1 be the P and Q tensors (3) and (4) for a cylindrical inclusion similar to a typical fiber (phase 1) but whose stiffness is L. Also, let P_3 and Q_3 be the P and Q tensors for an inclusion similar to a typical "fiber" of phase 3, but whose stiffness is L. Then, the estimates of the concentration factors for phases 1 and 3 are, from (10) and (11),

$$\begin{aligned} A_1 &= [I + P_1(L_1 - L)]^{-1} \quad , \quad B_1 = [I + Q_1(M_1 - M)]^{-1} \; , \\ A_3 &= [I + P_3(L_3 - L)]^{-1} \quad , \quad B_3 = [I + Q_3(M_3 - M)]^{-1} \; . \end{aligned} \tag{16}$$

Thus overall stiffness and compliance tensors (15) are given by

$$L = L_2 + c_1(L_1-L_2)\left[I+P_1(L_1-L)\right]^{-1} + c_3(L_3-L_2)\left[I+P_3(L_3-L)\right]^{-1}, \tag{17}$$

$$M = M_2 + c_1(M_1-M_2)\left[I+Q_1(M_1-M)\right]^{-1} + c_3(M_3-M_2)\left[I+Q_3(M_3-M)\right]^{-1}, \tag{18}$$

with $P_rL+Q_rM=I \quad (r=1,3)$.

We emphasize that the self-consistent method does not give direct estimates of A_2 or B_2. On the contrary, these factors must be found from (14). Thus the relationship between average matrix stress and the overall stress is written as

$$\bar{\underset{\sim}{\sigma}}_2 = B_2\bar{\underset{\sim}{\sigma}} = \frac{1}{c_2}(I-c_1B_1-c_3B_3)\bar{\underset{\sim}{\sigma}} \ . \tag{19}$$

Likewise, the average matrix strain is obtained from

$$\bar{\underset{\sim}{\varepsilon}}_2 = M_2\bar{\underset{\sim}{\sigma}}_2 = \frac{1}{c_2}M_2(I-c_1B_1-c_3B_3)L\bar{\underset{\sim}{\varepsilon}} \ . \tag{20}$$

Alternatively, in terms of strain concentration factors,

$$\bar{\underset{\sim}{\varepsilon}}_2 = A_2\bar{\underset{\sim}{\varepsilon}} = \frac{1}{c_2}(I-c_1A_1-c_3A_3)\bar{\underset{\sim}{\varepsilon}} \ , \tag{21}$$

$$\bar{\underset{\sim}{\sigma}}_2 = L_2\bar{\underset{\sim}{\varepsilon}}_2 = \frac{1}{c_2}L_2(I-c_1A_1-c_3A_3)M\bar{\underset{\sim}{\sigma}} \ . \tag{22}$$

3.b. Three Phase System with Cracks

We now show how the preceding theory is modified when we consider unidirectional fiber reinforced composites containing aligned slit cracks, see Figure 1a. First,

suppose that phase 3 consists of voids, so let $M_3 \to \infty$, $L_3 \to 0$. From (13) we now have

$$L = c_1 L_1 A_1 + c_2 L_2 A_2 \quad , \tag{23}$$

where, according to (16)

$$A_3 = [I - P_3 L]^{-1} = Q_3^{-1} L \quad . \tag{24}$$

Hence, A_2 in (21) now reduces to

$$A_2 = \frac{1}{c_2}(I - c_1 A_1 - c_3 Q_3^{-1} L) \quad , \tag{25}$$

and the overall stiffness for the composite with voids becomes, from (17),

$$L = L_2 + c_1 (L_1 - L_2) [I + P_1 (L_1 - L)]^{-1} - c_3 L_2 Q_3^{-1} L \quad . \tag{26}$$

Similarly, from (18)

$$M = M_2 + c_1 (M_1 - M_2) [I + Q_1 (M_1 - M)]^{-1} + c_3 Q_3^{-1} \quad . \tag{27}$$

In addition, the concentration factors for the average matrix stresses and strains are now given by

$$\bar{\underset{\sim}{\sigma}}_2 = \frac{1}{c_2}(I - c_1 B_1)\bar{\underset{\sim}{\sigma}} \quad , \tag{28}$$

$$\bar{\underset{\sim}{\varepsilon}}_2 = \frac{1}{c_2} M_2 (I - c_1 B_1) L \bar{\underset{\sim}{\varepsilon}} \quad , \tag{29}$$

as can easily be established from (19) and (20). Alternatively, the average stresses and strains in the matrix can be found from (21) and (22) providing that A_3 is taken from (24).

In order to make the transition from elliptic voids to slit cracks we recall that a and b are respectively the half-length and thickness of the elliptic voids (2). Let η be the number of voids per unit area of the x_1x_2-plane. Then the volume fraction of voids is

$$c_3 = \pi ab\eta \text{ ,}$$

or, according to (12),

$$\begin{aligned} c_3 &= \pi a^2\eta\delta \\ &= \tfrac{1}{4}\pi\beta\delta \end{aligned} \tag{30}$$

where $\beta = 4\eta a^2$ is the crack density parameter. Thus β is just the average number of cracks of length 2a in a square of side 2a. For example, in the crack patterns of Figures 1b and 1c, β measures the distance between regularly spaced cracks in terms of the crack length or ply thickness 2a. When $\beta = 1$ the distance between cracks is 2a, as β decreases the distance between cracks increases, and when $\beta = 0$ the cracks are no longer present. We note that experimental data [1-4] indicate the appropriate range for the crack density parameter is $0 \leq \beta < 1$.

We now turn our attention to equations (26) and (27) which, after a substitution for c_3 from (30), contain the term δQ_3^{-1}. The limit of this term for $\delta \to 0$ has already been considered by Eshelby [17], and more generally by Laws [15]. It turns out that while Q_3 becomes singular as $\delta \to 0$, the product δQ_3^{-1} remains finite:

$$\lim_{\delta \to 0} \delta Q_3^{-1} = \Lambda \quad . \tag{31}$$

In fact, for the material considered here the explicit form of Λ has been given by Laws [15]. We can now rewrite (26) and (27) for cracks using (31). The resulting expressions for overall stiffness and compliance of the cracked fibrous medium are

$$L = L_2 + c_1(L_1 - L_2)\left[I + P_1(L_1 - L)\right]^{-1} - \tfrac{1}{4}\pi\beta L_2\Lambda \quad , \tag{32}$$

$$M = M_2 + c_1(M_1 - M_2)\left[I + Q_1(M_1 - M)\right]^{-1} + \tfrac{1}{4}\pi\beta\Lambda \quad . \tag{33}$$

The matrix stress and strain concentration factor tensors are still given by (28) and (29), together with (16).

In the applications of the theory presented here we are concerned with matrices and fibers which are, at worst, transversely isotropic with respect to the fiber axis. Furthermore the geometry of the crack systems, Figure 1, is sufficiently simple to ensure that the overall composite is orthotropic. The components of Λ for such systems have been found explicitly by Laws [15]. It turns out that there are essentially three non-zero components of the Λ tensor. With the usual notation for the components of L, $L_{1111} = L_{11}$, $L_{1213} = L_{65}$ etc., it may be shown [15] that

$$\Lambda_{1212} = \frac{(L_{11}L_{22})^{\frac{1}{2}}(\alpha_1^{\frac{1}{2}}+\alpha_2^{\frac{1}{2}})}{4(L_{11}L_{22}-L_{12}^2)} ,$$

$$\Lambda_{2222} = \frac{L_{11}(\alpha_1^{\frac{1}{2}}+\alpha_2^{\frac{1}{2}})}{L_{11}L_{22}-L_{12}^2} , \qquad (34)$$

$$\Lambda_{2323} = \frac{1}{4(L_{44}L_{55})^{\frac{1}{2}}} ,$$

where α_1, α_2 are the roots of

$$L_{11}L_{66}\alpha^2 - (L_{11}L_{22}-L_{12}^2-2L_{12}L_{66})\alpha + L_{22}L_{66} = 0.$$

We note that the components of the P_1 tensor in (32) for the cylindrical fiber in an orthotropic effective medium are best evaluated by numerical integration of (3).

For a given concentration of fibers and given crack density, equations (32) or (33) provide a set of scalar equations for the overall moduli of the cracked composite. While it is possible, but tedious, to write down the component forms of these equations, it is much easier to solve (32) or (33) by using the tensor or matrix forms.

3.c. Two Phase System with Cracks

When the fiber diameters are very small compared with the crack length or ply thickness 2a, Figure 1c, it is physically reasonable to consider the possibility of modelling the effect of cracks in a fiber reinforced material by considering the fibers and matrix as a single-phase effective medium which contains cracks. To do so, we regard the fibrous composite as a new phase 2. Phase 1 is no longer present, while cracks retain their designation as phase 3. Thus, from (32) and (33)

$$L = L_2 - \tfrac{1}{4}\pi\beta L_2 \Lambda L \quad , \tag{35}$$

$$M = M_2 + \tfrac{1}{4}\pi\beta\Lambda \quad , \tag{36}$$

where L_2, M_2 now refer to the effective (uncracked) fibrous composite.

We shall refer to two different models of the fibrous composite with cracks: The model specified by (32) and (33) will be designated the three-phase model, whereas the model given by (35) and (36) will be called the two-phase model. In either case the formal theory is complete once the components of Λ have been specified.

For the two phase model it is possible to give compact equations for the overall components of the compliances. To do so, we first recast the non-zero components of Λ in terms of the compliances M_{ij}. With the usual notation

$$M_{1122} = M_{12}, \quad 2M_{2231} = M_{25}, \quad 4M_{3131} = M_{55},$$

and so on, it may be shown that

$$\Lambda_{22} = \Lambda_{2222} = \frac{M_{22}M_{33}-M_{23}^2}{M_{33}} (\alpha_1^{\frac{1}{2}} + \alpha_2^{\frac{1}{2}}) \quad ,$$

$$\Lambda_{44} = 4\Lambda_{2323} = (M_{44}M_{55})^{\frac{1}{2}} \quad , \tag{37}$$

$$\Lambda_{66} = 4\Lambda_{1212} = \frac{(M_{22}M_{33}-M_{23}^2)^{\frac{1}{2}}(M_{11}M_{33}-M_{13}^2)^{\frac{1}{2}}}{M_{33}} (\alpha_1^{\frac{1}{2}} + \alpha_2^{\frac{1}{2}}),$$

where α_1 and α_2 are the roots of

$$(M_{22}M_{33}-M_{23}^2)\alpha^2 - \{M_{33}M_{66}+2(M_{12}M_{33} - M_{13}M_{23})\}\alpha$$
$$+ M_{11}M_{33} - M_{13}^2 = 0 . \tag{38}$$

It now follows from (36) and (37) that six compliances are unaffected by the introduction of cracks:

$$M_{11} = M_{11}^{(2)} \; , \; M_{33} = M_{33}^{(2)} \; , \; M_{55} = M_{55}^{(2)} ,$$
$$M_{12} = M_{12}^{(2)} \; , \; M_{13} = M_{13}^{(2)} \; , \; M_{23} = M_{23}^{(2)} , \tag{39}$$

where $M_{ij}^{(2)}$ are the components of the compliance M_2 of the uncracked fibrous composite. The only components of M_2 which are altered are to be found from

$$M_{22} = M_{22}^{(2)} + \tfrac{1}{4}\pi\beta\Lambda_{22} \ ,$$

$$M_{44} = M_{44}^{(2)} + \tfrac{1}{4}\pi\beta\Lambda_{44} \ , \qquad (40)$$

$$M_{66} = M_{66}^{(2)} + \tfrac{1}{4}\pi\beta\Lambda_{66} \ .$$

From $(37)_2$, (39) and $(40)_2$ we may show that the overall transverse shear compliance M_{44} is given by the positive root of the quadratic equation:

$$M_{44} - \tfrac{1}{4}\pi\beta(M_{44}M_{55}^{(2)})^{\frac{1}{2}} - M_{44}^{(2)} = 0 \ . \qquad (41)$$

A particularly simple solution may be obtained for a dilute concentration of aligned slit cracks in an isotropic matrix. From (38) it follows that

$$\alpha_1 = \alpha_2 = 1.$$

Next, let E_m and ν_m be Young's modulus and Poisson's ratio for the matrix. Then, from (37) and (47), we have

$$M_{22} = \frac{1}{E_m}\{1 + \tfrac{1}{2}\pi\beta(1 - \nu_m^2)\} \ ,$$

$$M_{44} = \frac{2(1 + \nu_m)}{E_m}(1 + \tfrac{1}{4}\pi\beta) \ , \qquad (42)$$

$$M_{66} = \frac{2(1 + \nu_m)}{E_m}\{1 + \tfrac{1}{4}\pi\beta(1 - \nu_m)\} \ .$$

The remaining components of the compliance tensor of the cracked material are equal to those of the matrix.

The two phase model was proposed two decades ago by Bristow [6] in an attempt to quantify the behaviour of annealed and heavily cold-worked metals containing microcracks. In more recent years the two phase model has been the subject of deeper investigations by Budiansky and O'Connell [8] and Hoenig [9] amongst others. It is gratifying to note that (36) agrees with a corresponding equation (2.14) in Hoenig's paper [9]. Likewise, if we were to allow for nonalignment of the cracks, (36) would reduce to the scalar equations derived by Budiansky and O'Connell [8] for randomly oriented cracks in an isotropic matrix. Furthermore, equations (42) imply Bristow's [6] results for dilute distributions of cracks.

4. NUMERICAL EVALUATION OF L

The numerical evaluation of L is achieved by the following iterative method. First, we rewrite (32) as

$$L = F(\beta, c_1, L) ,$$

where

$$F(\beta, c_1, L) =$$

$$[I + \tfrac{1}{4}\pi\beta L_2 \Lambda]^{-1}\{L_2 + c_1(L_1 - L_2)[I + P_1(L_1 - L)]^{-1}\} .$$

The iteration commences with

$$L^{(1)} = L_2 ,$$

and successive iterates are obtained from

$$L^{(k+1)} = \tfrac{1}{2}(S^{(k)} + S^{(k)T}); (k \geq 1) ,$$

where

$$S^{(k)} = F(\beta, c_1, L^{(k)}) .$$

This iteration scheme is repeated until a particular convergence criterion is satisfied. In the results that follow we used the criterion

$$\frac{\| L^{(k+1)} - L^{(k)} \|}{\| L^{(k)} \|} \leq \varepsilon$$

where ε is a suitable error bound - say 10^{-3}.

It is probably obvious from material symmetry considerations that the resulting L for the cracked medium has nine independent coefficients, in contrast to the five moduli which appear in the stiffness tensor of the uncracked fibrous composite. This is indeed borne out in the numerical solution of (32).

It is, perhaps, important to emphasize that the present approach does not distinguish between cracks opening or closing. We expect our results only to be valid when the cracks are open - and note that the quantification of this statement is nontrivial except when the applied normal strains are all positive.

5. RESULTS FOR SELECTED MATERIAL SYSTEMS

To illustrate the effect of matrix cracking on the properties of typical composite systems, we present results of numerical solutions of Equations (32) and (35). The material systems considered are a graphite-epoxy composite, and a boron-aluminum composite. The elastic properties of the fibers and matrices were taken as:

VS 0054 Gr/Ep:

	Unit	E_{33}	G_{31}	ν_{31}	E_{11}	G_{12}	Symmetry
Fiber	10^3 ksi	100.00	2.20	0.00495	1.10	0.38	Transversely Isotropic
	10^3 MPa	689.5	15.2		7.6	2.6	
Matrix	10^3 ksi	0.50	0.19	0.20980	0.50	0.19	Isotropic
	10^3 MPa	3.4	1.3		3.4	1.3	

B/Aℓ:

	Unit	E	G	Symmetry
Fiber	10^3 ksi	58.00	23.97	Isotropic
	10^3 MPa	399.9	165.3	
Matrix	10^3 ksi	10.50	3.95	Isotropic
	10^3 MPa	72.4	27.2	

Interpretation of results should be facilitated by an explicit display of the overall stiffness. Hence we rewrite (1) for the cracked medium in matrix form:

$$\underset{\sim}{\sigma} = L \underset{\sim}{\varepsilon}$$

$$\begin{bmatrix} \sigma_{11} \\ \sigma_{22} \\ \sigma_{33} \\ \sigma_{23} \\ \sigma_{13} \\ \sigma_{12} \end{bmatrix} = \begin{bmatrix} L_{11} & L_{12} & L_{13} & 0 & 0 & 0 \\ & L_{22} & L_{23} & 0 & 0 & 0 \\ & & L_{33} & 0 & 0 & 0 \\ & & & L_{44} & 0 & 0 \\ & & & & L_{55} & 0 \\ \text{SYM.} & & & & & L_{66} \end{bmatrix} \begin{bmatrix} \varepsilon_{11} \\ \varepsilon_{22} \\ \varepsilon_{33} \\ 2\varepsilon_{23} \\ 2\varepsilon_{13} \\ 2\varepsilon_{12} \end{bmatrix} . \qquad (43)$$

Figures 2a to 2i show the results obtained for the graphite/epoxy system. Calculations were made for three different volume fractions $c_1 = c_f$ of the fiber, both with the two-phase and three-phase model. This was done to highlight the differences in results obtained from the two models. Since the diameter of graphite fibers is usually of the order of 1μ, there are many fibers in each ply of a laminated structure, and therefore, the cracks will be much larger than the fiber diameter. Accordingly, the two-phase model of Figure 1c will be more appropriate for this system.

Figures 3a to 3i show the results obtained for the boron/aluminum system. Again, three values of $c_1 = c_f$ were selected. In contrast to the graphite fiber, the boron filament is usually of large diameter, 150μ or so, and only one layer of fibers is present in a typical ply. The crack length is then comparable to the fiber diameter, and the three-phase model is the appropriate one for this composite system. Again, results for both models are presented.

It is seen that the presence of cracks has a very similar effect on the individual coefficients of L_{ij} in both material systems. However, specific L_{ij} components change in different ways. For both systems, L_{11}, L_{12}, L_{13}, L_{22}, and L_{23} reduce quite rapidly with increasing β^+. On the other hand, L_{33} is essentially constant in graphite-epoxy, but decreases slowly in boron-aluminum. Finally, the shear stiffnesses for both systems decrease rather slowly.

It is of interest to discuss the results in terms of the respective Young's moduli and Poisson's ratios. Thus we write the inverse of equation (43) in the form

$$\begin{bmatrix} \varepsilon_{11} \\ \varepsilon_{22} \\ \varepsilon_{33} \\ 2\varepsilon_{23} \\ 2\varepsilon_{13} \\ 2\varepsilon_{12} \end{bmatrix} = \begin{bmatrix} \frac{1}{E_{11}} & -\frac{\nu_{12}}{E_{11}} & -\frac{\nu_{13}}{E_{11}} & 0 & 0 & 0 \\ -\frac{\nu_{21}}{E_{22}} & \frac{1}{E_{22}} & -\frac{\nu_{23}}{E_{22}} & 0 & 0 & 0 \\ -\frac{\nu_{31}}{E_{33}} & -\frac{\nu_{32}}{E_{33}} & \frac{1}{E_{33}} & 0 & 0 & 0 \\ 0 & 0 & 0 & \frac{1}{L_{44}} & 0 & 0 \\ 0 & 0 & 0 & 0 & \frac{1}{L_{55}} & 0 \\ 0 & 0 & 0 & 0 & 0 & \frac{1}{L_{66}} \end{bmatrix} \begin{bmatrix} \sigma_{11} \\ \sigma_{22} \\ \sigma_{33} \\ \sigma_{23} \\ \sigma_{13} \\ \sigma_{12} \end{bmatrix}$$

+ Recall that the distance between cracks is equal to $2a/\beta$, where $2a$ is crack length or ply thickness, Figures 1b, c.

First, it is significant that E_{11}, E_{33}, ν_{12}, ν_{13}, ν_{31}, and ν_{32} are virtually independent of the crack density parameter β. Correspondingly, the choice of the two or three phase model is irrelevant. Second, the moduli E_{22}, ν_{21}, and ν_{23} exhibit significant dependence on β, as is displayed in Figure 4 and 5. Moreover, the difference between the two and three phase models is again minimal for $c_f \leq 0.4$. As far as the shear moduli L_{44} and L_{55} are concerned, the predictions of the two and three phase models are different, c.f., Figure 2g, 2h, 3g, 3h. Also, L_{44} and L_{66} depend strongly on β, whereas L_{55} does not.

Finally we note that the cracks cause a much larger absolute reduction of many overall stiffness coefficients in the metal matrix system than they do in the polymer system. This is to be expected on the basis of matrix and fiber properties shown above. The epoxy matrix has a very low stiffness even in the undamaged state, and the fiber has a low transverse modulus. The overall stiffnesses of the Gr/Ep system (except for L_{33}) shown in Figure 3 are one order of magnitude smaller than those of the B/Aℓ system in Figure 2. Therefore, the Gr/Ep composite properties leave only limited room for reduction by matrix cracking.

ACKNOWLEDGEMENT

This work has been supported by a grant from the Air Force Office of Scientific Research.

CAPTIONS

Figure 1a. A three-phase medium with aligned fibers and longitudinal slit cracks in a continuous matrix.

Figure 1b. A filament monolayer with longitudinal slit cracks.

Figure 1c. A lamina containing small diameter fibers and longitudinal slit cracks.

Figure 2. Stiffness changes caused by a system of longitudinal slit cracks in a Gr/Ep composite.

Figure 3. Stiffness changes caused by a system of longitudinal slit cracks in a B/Aℓ composite.

Figure 4. Young's modulus and Poisson's ratios of the Gr/Ep system, which change with crack density parameter β.

Figure 5. Young's modulus and Poisson's ratios of the B/Aℓ system which change with crack density parameter β.

REFERENCES

1. Dvorak, G. J., and Johnson, W. S., "Fatigue of Metal Matrix Composites," Intl. J. Fracture, Vol. 16, 1980, pp. 585-607.
2. Dvorak, G. J., and Johnson, W. S., "Fatigue Mechanisms in Metal Matrix Composite Laminates," Advances in Aerospace Structures and Materials, ASME, AD-01, 1981, pp. 21-34.
3. Reifsnider, K. L., and Talug, A., "Analysis of Fatigue Damage in Composite Laminates," Intl. J. Fatigue, 1980, p. 3.
4. Bader, M. G., Bailey, J. E., Curtis, P. T., and Parvizi, A., "The Mechanisms of Initiation and Development of Damage in Multi-Axial Fiber-Reinforced Plastic Laminates," Proceedings of Third International Conference on Mechanical Behavior of Materials, Cambridge, 1979, p. 227.
5. White, M. K., and Wright, M. A., "The Fatigue Properties of Cross-Plied Boron 6061 Aluminum," J. Materials Sci., Vol. 14, 1979, pp. 653-662.
6. Bristow, J. R., "Microcracks, and the Static and Dynamic Elastic Constants of Annealed and Heavily Cold-Worked Metals," Brit. J. Appl. Phys., Vol. 11, 1960, pp. 81-85.
7. Walsh, J. B., "New Analysis of Attenuation in Partially Melted Rock," J. Geophys. Res., Vol. 74, 1969, pp. 4333-4337.
8. Budiansky, B., and O'Connell, R. J., "Elastic Moduli of a Cracked Solid," Intl. J. Solids Structures, Vol. 12, 1976, pp. 81-97.
9. Hoenig, A., "Elastic Moduli of a Nonrandomly Cracked Body," Intl. J. Solids Structures, Vol. 15, 1979, pp. 137-154.

10. Willis, J. R., "Bounds and Self-Consistent Estimates for the Overall Properties of Anisotropic Composites," J. Mech. Phys. Solids, Vol. 25, 1977, pp. 185-202.

11. Taya, M., and Mura, T., "On Stiffness and Strength of an Aligned Short-Fiber Reinforced Composite Under Uniaxial Applied Stress When the Composite Contains Fiber End Cracks," J. Appl. Mech., Vol. 48, 1981, pp. 361-367.

12. Delameter, W. R., Herrmann, G., and Barnett, D. M., "Weakening of an Elastic Solid by a Rectangular Array of Cracks," J. Appl. Mech., Vol. 42, 1975, pp. 74-80, Vol. 44, 1977, p. 190.

13. Hill, R., "Elastic Properties of Reinforced Solids: Some Theoretical Principles," J. Mech. Phys. Solids, Vol. 11, 1963, pp. 357-372.

14. Kinoshita, N., and Mura, T., "Elastic Fields of Inclusions in Anisotropic Media," Phys. Stat. Sol. (a), Vol. 5, 1971, pp. 759-768.

15. Laws, N., "A Note on Interaction Energies Associated with Cracks in Anisotropic Media," Phil. Mag., Vol. 36, 1977, pp. 367-372.

16. Hill, R., "A Self-Consistent Mechanics of Composite Materials," J. Mech. Phys. Solids, Vol. 13, 1965, pp. 213-222.

17. Eshelby, J. D., "The Determination of the Elastic Field of an Ellipsoidal Inclusion and Related Problems," Proc. Roy. Soc., Ser. A, Vol. 241, 1957, pp. 376-396.

18. Eshelby, J. D., "Elastic Inclusions and Inhomogeneities," in Progress in Solid Mechanics, Vol. 2, I. N. Sneddon and R. Hill, editors. North-Holland, Amsterdam, 1961, Chapter III, pp. 89-140.

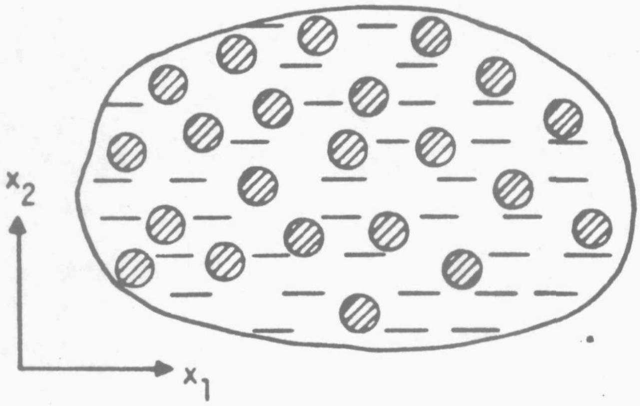

Figure 1a.

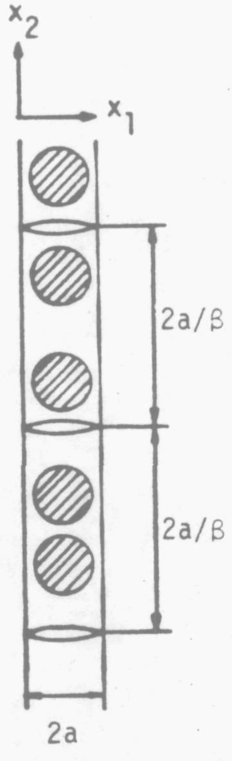

Figure 1b.

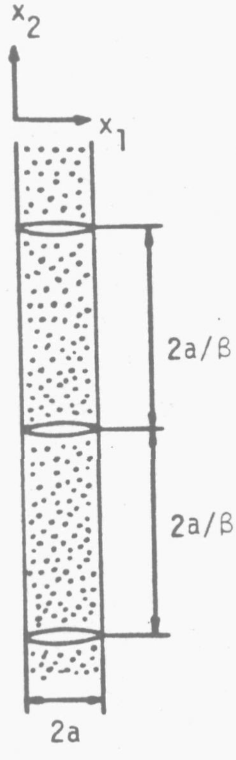

Figure 1c.

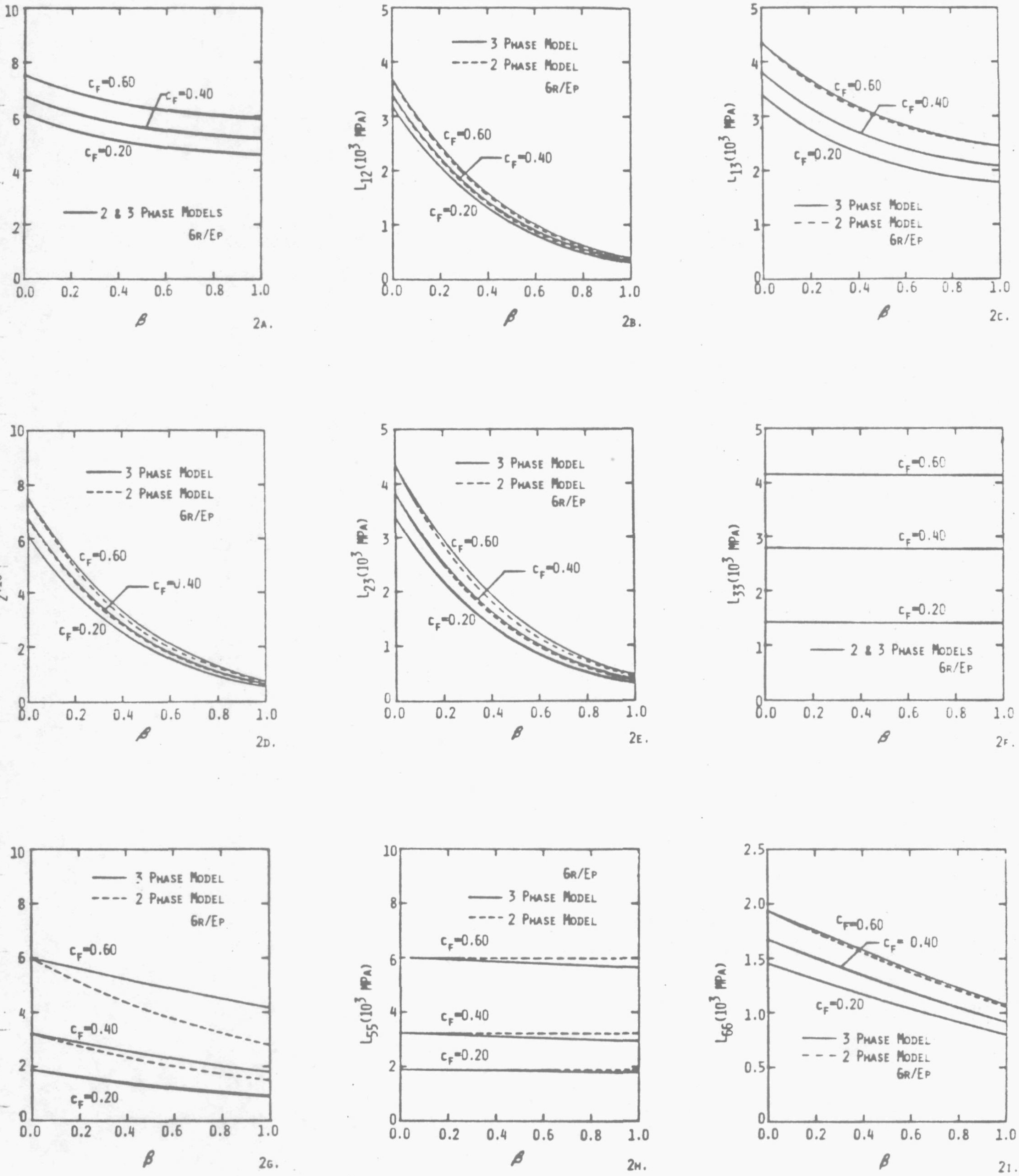

Figure 2. Stiffness changes caused by a system of longitudinal slit cracks in a Gr/Ep composite.

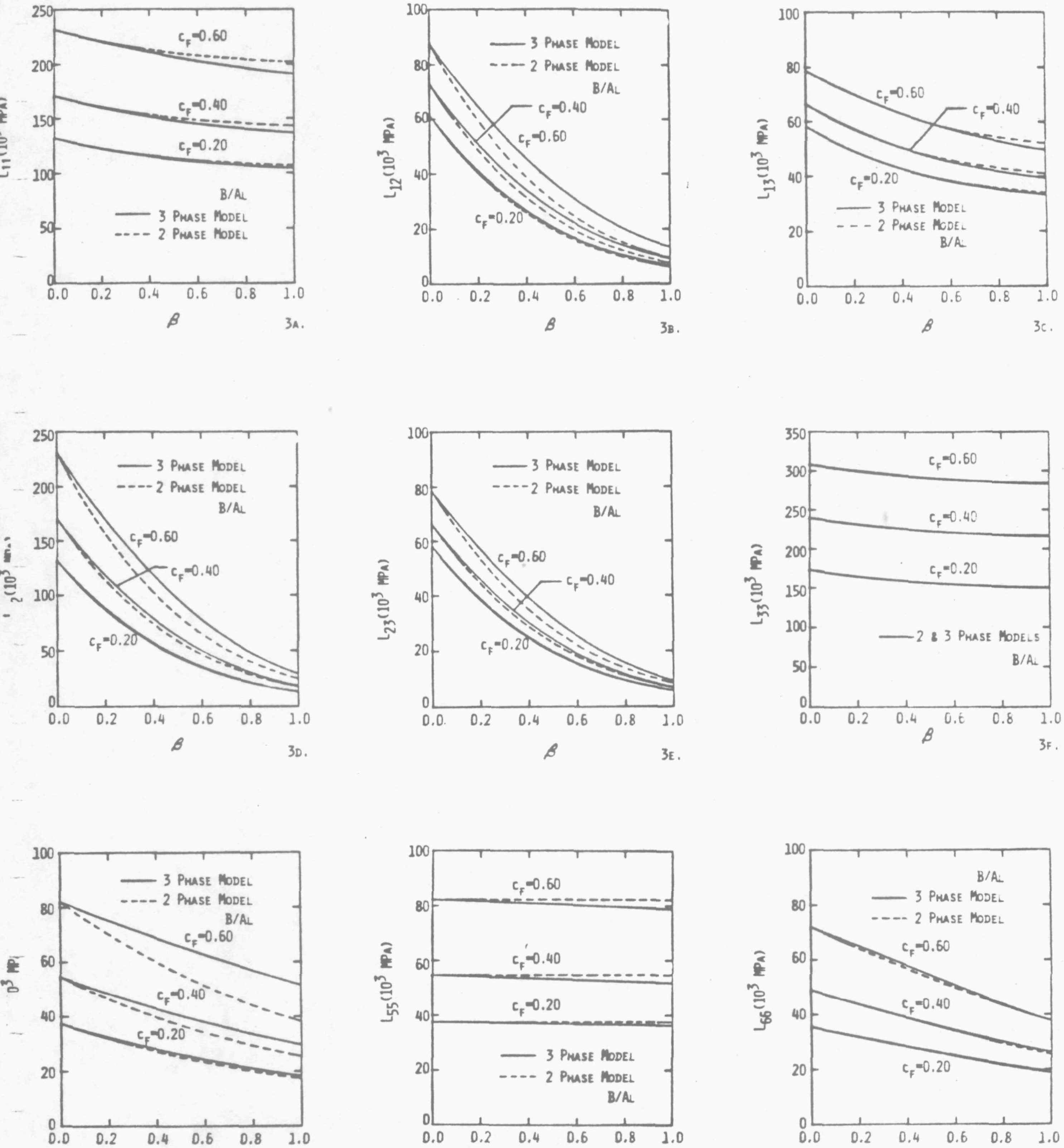

Figure 3. Stiffness changes caused by a system of longitudinal slit cracks in a B/Aℓ composite.

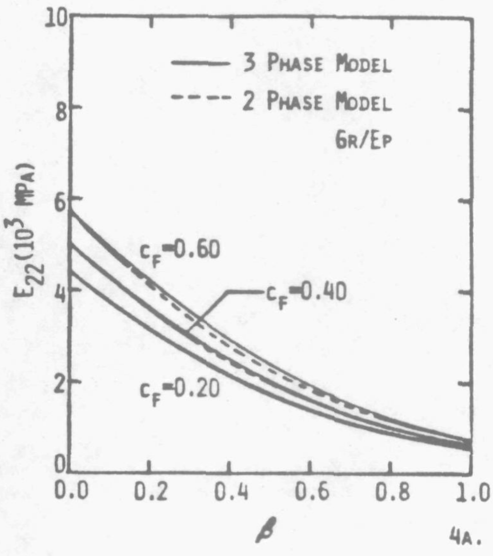

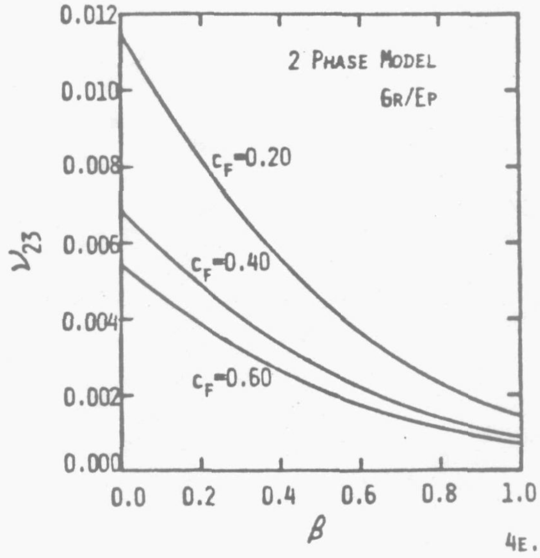

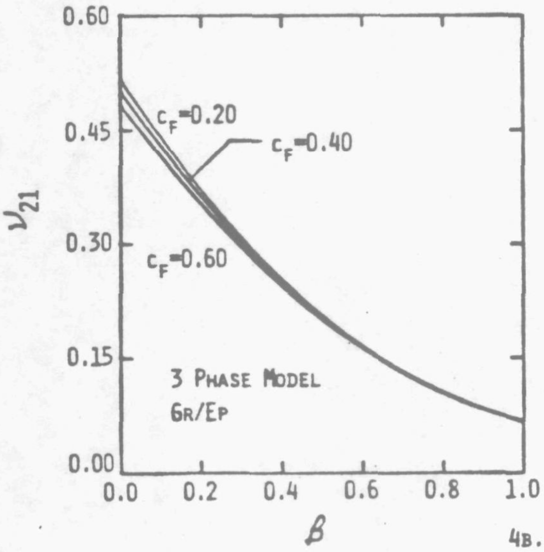

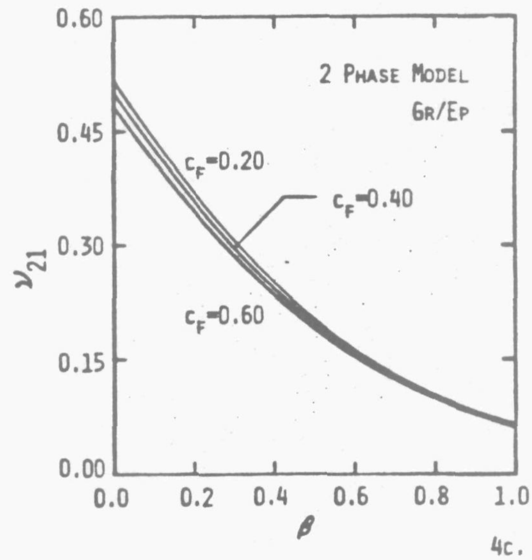

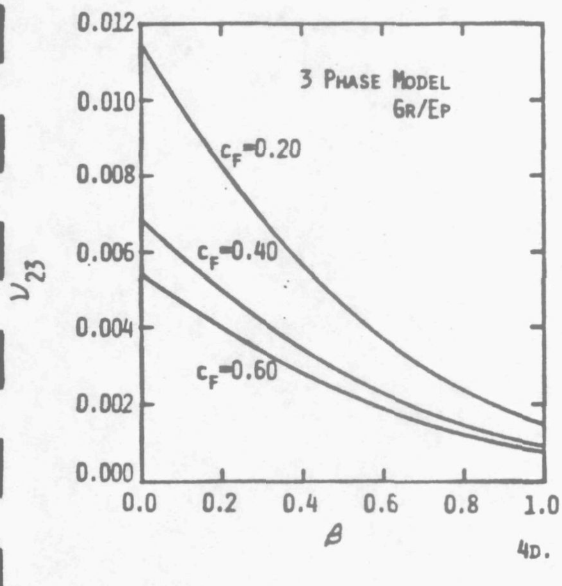

Figure 4. Young's modulus and Poisson's ratios of the Gr/Ep system which change with crack density parameter β.

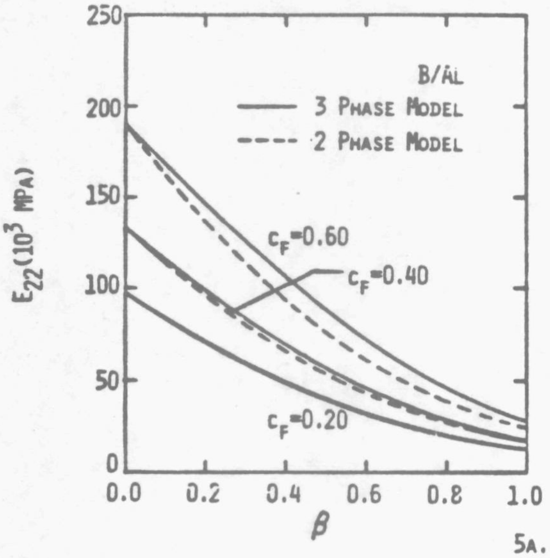

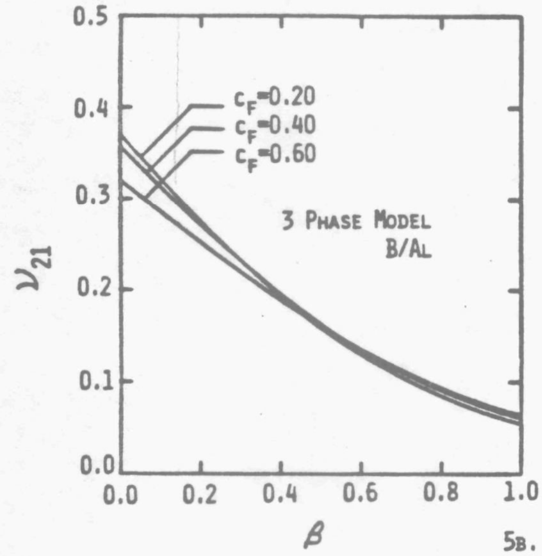

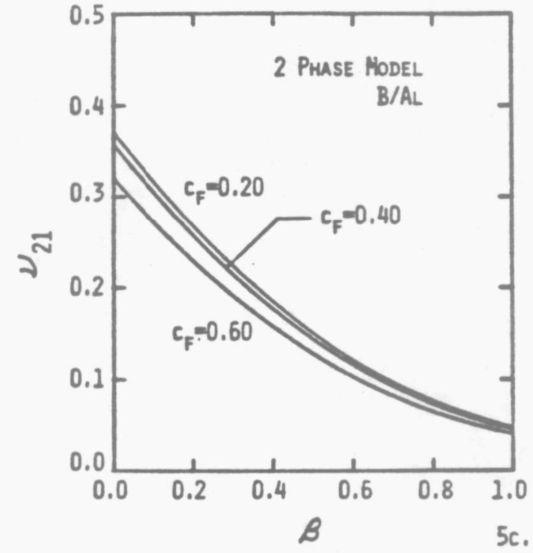

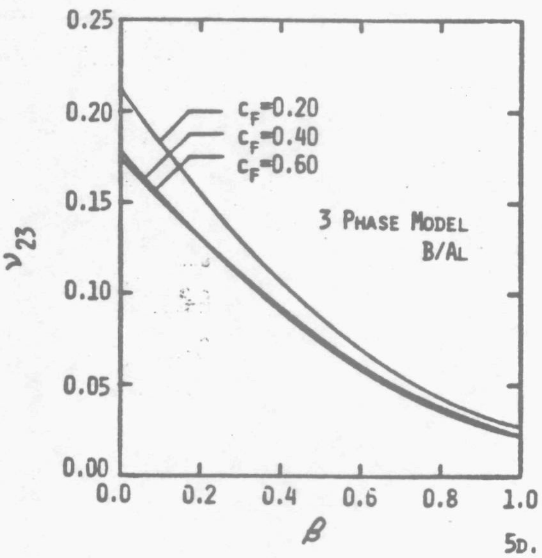

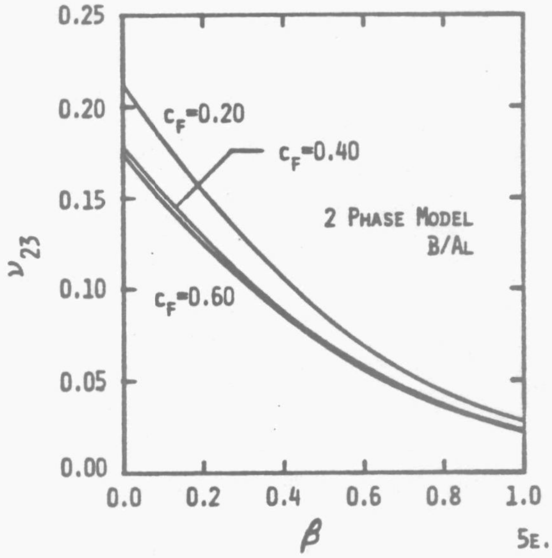

Figure 5. Young's modulus and Poisson's ratios of the B/Aℓ system which change with crack density parameter β.